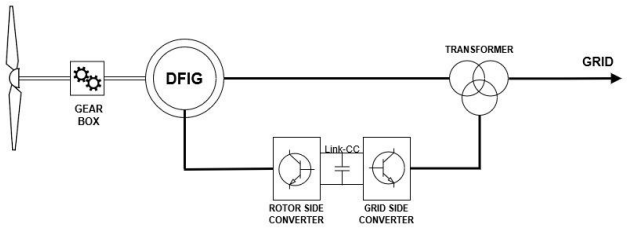

Figure 5 – Doubly-fed induction generator

The DFIG model has gained importance due to the technological advances in the power electronics area, and the development of vector control techniques. This arrangement allows the decoupling between active and reactive power, as well as the generation of power at rated frequency and voltage regardless of the rotor speed [25], [26].

The back-to-back converter controls the power flow between the rotor and the grid. This converter consists of two inverters with Insulated Gate Bipolar Transistors (IGBTs), sharing a direct current link as illustrated in Figure 6 [25], [26].

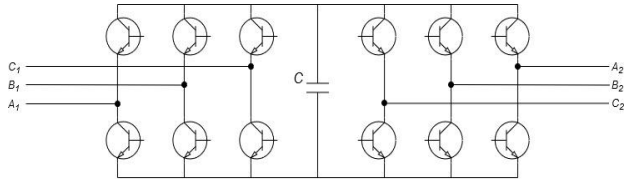

Figure 6 – Back-to-back converter circuit

In this work, the detailed back-to-back converter model was implemented. In other words, the IGBTs keys were properly represented as illustrated in Figure 6.

For proper operation of this converter two control systems are required, namely the Rotor Side converter Controller (RSC), and the Grid Side converter Controller (GSC). RSC is responsible for control the active and reactive powers provided by the wind generator, while GSC is responsible for maintaining constant DC-link voltage, to provide reactive power support, and to control the power exchange between the grid and the converter. More information about these controllers can be found in [25], [26].

C. Energy Storage System

The battery model used was the Li-Ion Battery technology – which is present in the RSCAD library – connected to the network via a Voltage Source Converter (VSC).

The VSC was implemented using an averaged model with dependent sources, as illustrated in Figure 7. As it neglects the effects of thyristor switching [27], the averaged model was used due to the processing limitations of the real-time simulation structure available for testing.

According to [27], although it is not a true representation of the DC/AC converter, the model used does not show significant losses when compared to the detailed model if the microgrid operates under load and with balanced conditions.

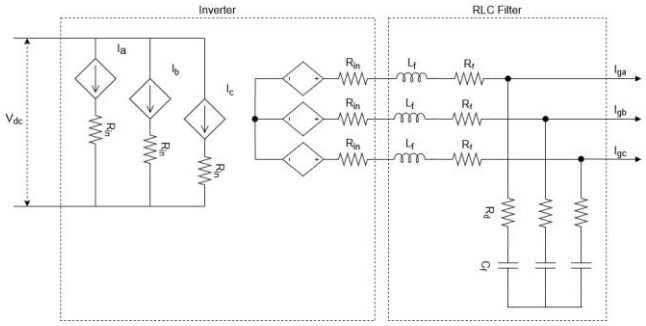

Figure 7 – Back-to-back converter circuit

The used battery control is based on the d-q axis decoupling for the control of the active and reactive power supplied to the grid. Figure 8 illustrates the block diagram of the battery control.

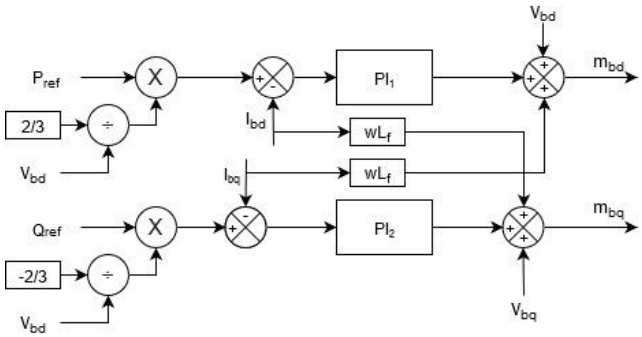

Figure 8 – Block diagram of the battery control

D. Transmission Lines

Due to their small lengths, the transmission lines were modeled using their PI equivalents. The electrical parameters of the lines can be found in [22].

E. Loads

All loads of the microgrid are three-phase, balanced and were modeled as dynamic loads. This model is available in RSCAD software package. The electrical parameters of the lines can be found in [22].

5. Tests and Results

In this section, the results obtained from the initial tests performed in the implemented microgrid are shown. Due to processing limitations, the global simulation time-step was set to 90μs. Furthermore, it was adjusted a sub-time step of 3.6μs to simulate the power electronics converters.

In order to analyze the dynamic performance of the system, three simulations of events held to test the implemented microgrid, which will be described below. In both simulations, the diesel generator supplied approximately 0.2MW of active power and 0.3Mvar of reactive power, the battery bank provided approximately 0.2MW of active power, and the wind generator approximately 0.7MW of active power.

Each simulation performed differs in the level of the load step applied at Bus 9. The load step applied in each simulation is presented in Table I.

Table I – Load steps for the simulated events

Simulation	Active Power [MW]	Reactive Power [MVar]
1	0.34	0.036
2	0.5	0.051
3	0.5	0.51

Also, it was considered that there is an extremely important load connected to bus 11, so this bus was considered the main bar of the system.

Figure 9 shows the results of frequency and voltage at bus 11 for the simulated events. It is verified that the microgrid is stable from the viewpoint of simulated events, and the electrical quantities reach adequate values after the perturbations. It is important to highlight that the results presented in Figure 9 can be externalized to test the equipment present in the control center (third layer) to define and validate the best control strategy.

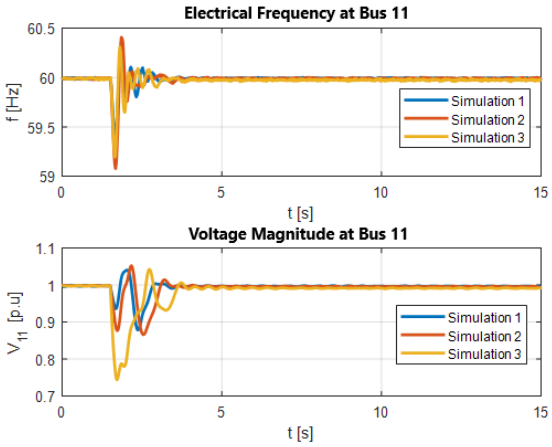

Figure 9 – System frequency and voltage at bus 11 for the simulated events

5. Conclusion

Because it is a multidisciplinary and highly complex theme, the complete understanding of the phenomena that permeate the concept of microgrids demands the application of sophisticated analysis tools. Within this context, this paper presented a comprehensive survey of the main tools used for this task.

Among the presented tools, emphasis is given to those involving the concept of HIL simulation. Through the use of real-time simulation platforms and by establishing appropriate interfaces between simulated and real parts of the system, the HIL concept allows equipment to be tested in conditions very close to those found field, with the advantage of analysis flexibility through the possibility of representation of different operational conditions.

The results from the presented example, which correspond to an actual implementation at the facility to which the first authors are affiliated, illustrated the previously mentioned advantages of having a flexible testbed for microgrid simulation.

Acknowledgement

We are grateful for the support of Itaipu Binacional and Itaipu Technological Park. This work is part of the research group "Microgrids and Systems with Distributed Generation by Real Time Simulation" (CNPQ) and "Hybrid Intelligent Electrical Microregions with High Penetration of Renewable Energies" (CYTED-717RT0533).

References

[1] R. H. Lasseter, “Microgrids”. IEEE Power Engineering Society Winter Meeting. (2002.) v. 1, p. 305–308 vol.1..

[2] A. B. Piardi, R. B. Otto , D. G. Sonoda, F. C. Santos, L.R.A Ferreira and R. A. Ramos, “Laboratory for Analysis of Microgrid with Real Time Simulation”, ICREPQ’19 (2019).

[3] Working Group C6.22 “Microgrids Evolution Roadmap, Microgrids 1 Engineering, Economics, & Experience” CIGRE (2015).

[4] A. Bani-Ahmed and A. Nasiri, "Development of Real-Time Hardware-in-the-Loop Platform for Complex Microgrids," ICRERA (2015), Palermo, pp. 994-998.

[5] A. B. Piardi, F. C. dos Santos, D. G. Sonoda, R. B. Otto, “Aspects of a Hybrid and Flexible Microgrid Laboratory Implementation”, XIV SEPOPE (2018).

[6] Marnay, C. et al. “Microgrid evolution roadmap”. EDST (2015). p. 139–144.

[7] N. Hatziargyriou, et al. “Microgrids”. IEEE Power and Energy Magazine (2007). v. 5, n. 4, p. 78–94.

[8] B. Xiao, et al. “Development of hardware-in-the-loop microgrid testbed”. IEEE Energy Conversion Congress and Exposition (2015).

[9] P. P. Domingues, et Al. “Uso de Software Livre em Atividades de Ensino e Pesquisa em Microeletrônica”. XLIV COBENGE (2016).

[10] RTDS Technologies, “Microgrid Simulation and Testing”. Available in: < https://www.rtds.com/ >. Access in 2019.11.11.

[11] D. P. Chassin, K. Scheneider, C. Gerkensmeyer. “Gridlab-D: An opensource power systems modeling and simulation environment”. T&D (2008). p. 1–5. ISSN 2160-8555.

[12] HOMER. HOMER PRO and HOMER GRID. 2019. Available in: < https://www.homerenergy.com >. Access in 2019.11.11

[13] MATLAB Simscape Electrical. 2019. Available in: < https://www.mathworks.com/products/simscapeelectrical.html >. Access in 2019.11.11

[14] EPRI. “Introduction to the OpenDSS”. (2009). Available in: <http:// https://www.epri.com/#/pages/sa/opendss?lang=en-US/>. Access in: 2019.11.11

[15] W. Ren, M. Steurer and T. L. Baldwin, "Improve the Stability and the Accuracy of Power Hardware-in-the-Loop Simulation by Selecting Appropriate Interface

Algorithms," in IEEE Transactions on Industry Applications, vol. 44, no. 4, pp. 1286-1294, July-Aug. 2008.
[16] J. Wang, Y. Song, W. Li, J. Guo and A. Monti, "Development of a Universal Platform for Hardware In-the-Loop Testing of Microgrids," in IEEE Transactions on Industrial Informatics, vol. 10, no. 4, pp. 2154-2165, Nov. 2014.
[17] PSCAD. "User´s Guide on the use of PSCAD" (2018). Available in: <https://hvdc.ca/uploads/knowledge base/pscad manual v4 6.pdf?t=1528395602>. Access in: 2019.11.13
[18] OPAL-RT. "Simulator Platform Comparison Chart" (2019). Available in: <https://www.opalrt.com/wpcontent/themes/ enfold-opal/pdf/L00161 0472.pdf>. Access in: 2019.11.13
[19] OPAL-BROCHURE. "Real-Time Simulation Solutions for Power Grids and Power Electronics" (2019). Available in: <https://www.opal-rt.com/wpcontent/themes/enfoldopal/pdf/ L001610260.pdf>. Access in: 2019.11.13
[20] OPAL-CHART. "Website da OPAL-RT" (2019). Available in: <https://www.opal-rt.com/>. Access in: 2019.11.13
[21] TYPHOON. Website da Typhoon HIL. 2019. Available in: <https://www.typhoon-hil.com/>. Access in: 2019.11.13
[22] CIGRE Task Force C6.04.02, Benchmark Systems for Network Integration of Renewable and Distributed Energy Resources. CIGRE, (2014).
[23] R. B. Otto, R. F. Espinoza, A. Piardi, and M. do Carmo. "Microgrid benchmark system: Rtds implementation,". Available in: <https://github.com/Itaipr/MICROGRID-RTDS> (2019)
[24] "IEEE recommended practice for excitation system models for power system stability studies," *IEEE Std 421.5-2016 (Revision of Std 421.5-2005)*, pp. 1–207, Aug 2016.
[25] G. Abad, J. Lopez, M. Rodriguez, L. Marroyo, and G. Iwanski, *Doubly fed induction machine: modeling and control for wind energy generation*.
[26] H. Abu-Rub, M. Malinowski, and K. Al-Haddad, *Power electronics for renewable energy systems, transportation and industrial applications.*
[27] M. Farrokhabadi, S. Konig, C. A. Canizares, K. Bhattacharya, and T. Leibfried, "Battery energy storage system models for microgrid stability analysis and dynamic simulation," *IEEE Transactions on Power Systems*, vol. 33, no. 2, pp. 2301–2312, March 2018.